High-temperature electron emission from diamond films

S. H. Shin
Department of Mechanical Engineering, Vanderbilt University, Nashville, Tennessee 37235

T. S. Fisher[a)]
School of Mechanical Engineering and Birck Nanotechnology Center, Purdue University, West Lafayette, Indiana 47907-1288

D. G. Walker and A. M. Strauss
Department of Mechanical Engineering, Vanderbilt University, Nashville, Tennessee 37235

W. P. Kang and J. L. Davidson
Department of Electrical Engineering and Computer Science, Vanderbilt University, Nashville, Tennessee 37235

(Received 3 April 2002; accepted 18 November 2002; published 5 February 2003)

This work examines electron field-emission characteristics of polycrystalline diamond films at elevated temperatures. Diamond is an excellent material as a field emitter because of its exceptional mechanical hardness and chemical inertness. The motivation behind this study involves the use of field emitters in applications where high temperatures exist. Nitrogen-doped polycrystalline diamond films were grown by plasma-enhanced chemical-vapor deposition. To investigate the effect of increased temperatures on field emission, current–voltage measurements were taken from the same diamond film at varying temperatures. Results from these measurements indicate a decrease in the turn-on voltage with increasing temperature. Further analysis of the temperature dependence of emission is achieved through parameter estimation of the effective emitting area, field enhancement factor, and work function. These results suggest that thermally excited electrons are responsible for improved emission at high temperature. © *2003 American Vacuum Society.*
[DOI: 10.1116/1.1537231]

I. INTRODUCTION

In recent years, chemical-vapor deposited (CVD) diamond has attracted considerable interest for use as an electron emitter due to its low-field-emission characteristics. Diamond films have important advantages over other field-emission materials, including chemical stability, mechanical hardness, and high thermal conductivity. In the present work, experimental results are interpreted in terms of the traditional Fowler–Nordheim (FN) theory and an alternative model that includes size and temperature effects explicitly. The comparison between the FN results and the alternative model elucidates the potential advantages of the latter for use in predicting high-temperature emission behavior.

High-temperature thermionic electron emission has been studied for several decades.[1] A fundamental understanding of thermionic emission was developed primarily from vacuum-tube transistors, which operate on the basis of electron emission over a potential barrier. Thermionic emission has also been used for direct thermal-to-electrical power generation. Thermionic energy conversion is inherently efficient due to the unimpeded flow of electrons through the vacuum and the elimination of heat conduction provided by the vacuum, leaving thermal radiation as the primary heat loss mechanism. However, the power generation capacity of traditional thermionic devices is limited by the relatively high work functions ($\sim$1.5 eV) of most metallic emitters. On the other hand, field-emission devices have exhibited low effective work functions, and show promise in direct energy conversion applications[1] using thermionic and/or field emission.

Fowler and Nordheim[2] provided the first theoretical treatment of field emission from planar metal surfaces. Spindt demonstrated that sharp geometric surface features enhance emission substantially.[3] The emission properties of a wide variety of metallic and semiconductor materials and structures have been studied in detail.[4,5] The emission properties of carbon-based/diamond materials, in particular, are very robust.[6] However, the physical reasons behind the outstanding emission properties of carbon-based materials remain the subject of scientific inquiry.[7] Suggested applications for field-emission devices include vacuum field-effect transistors, diodes and triodes, ion sources, electron guns, flat-panel displays, scanning microscopes, and many others.[4]

As an electron emitter, diamond can exhibit a low or even negative electron affinity (NEA) with appropriate surface termination.[8] This effect allows a reduction in the turn-on voltage required to achieve field emission by eliminating the potential barrier required to inject an electron from the conduction band into the vacuum.[9] NEA can, therefore, improve field emission when emitted electrons originate from the conduction band minimum.[10] With the absence of n-type doping, however, the concentration of electrons in the conduction band is negligible at thermal equilibrium due to the large band gap of diamond ($E_g = 5.45$ eV).[11]

Much research has been conducted to elucidate the exact

[a)]Author to whom correspondence should be addressed; electronic mail: tsfisher@purdue.edu

mechanism of field emission and to improve the performance of CVD polycrystalline diamond as an electron emitter. The present work considers high-temperature emission from diamond with the expectation that the temperature dependence will provide insight into the emission mechanism. The traditional FN theory and an alternate theory are used to interpret high-temperature emission data. The FN theory, which ignores temperature effects, produces estimates of emission parameters, such as work function and field enhancement factor, that vary significantly with temperature. The alternate theory, which includes temperature effects, is shown to predict parameters within a narrower, albeit still broad, range.

The objective of the current work is to identify parameters important to field emission in polycrystalline diamond through experimentation and parameter estimation. Also, the significance of temperature effects and the need to model them is highlighted. The following sections describe the theories of field emission and parameter estimation employed in the present work. Later sections describe the experimental methods and results compared to theoretical models.

II. FIELD-EMISSION THEORY

This study focuses on the high-temperature field-emission characteristics of polycrystalline diamond films for thermal–electrical energy conversion applications. Using the formulation of Good and Muller[12] for basic FN emission, current density can be expressed analytically as

$$I=\frac{1.5\times10^{-6}\beta^2F^2A}{\phi}\exp\left(\frac{10.4}{\phi}\right)\exp\left(\frac{-6.44\times10^{7}\phi^{3/2}}{\beta F}\right), \tag{1}$$

where I is the current (amp), A is the emission area (cm^2), F is the *average* applied electric field (V/cm), β is the field enhancement factor, and ϕ is an effective work function (eV). Note that temperature effects are absent.

Often, the FN expression is cast into a linear form

$$\ln\left(\frac{I}{F}\right)=c_0+c_1\left(\frac{1}{F}\right), \tag{2}$$

where the slope c_1 and intercept c_0 can be found using a simple linear regression. The three model parameters (work function, emission area, and enhancement factor) cannot be determined uniquely from current–voltage ($I-V$) behavior. The following section describes the method of estimating these parameters.

In the present work, we employ an alternate model that is more physically accurate than the basic FN approach. The model was described in a recent paper[13] and is summarized here for clarity. The model includes two important features that improve the physicality of the FN model. The temperature dependence of the electrons available for emission provides more accuracy in simulating the thermodynamics of field emission. In addition, the curvature of the one-dimensional potential field is described with the inclusion of curvature due to geometric features, instead of the field enhancement factor used in the FN formulation. Other detailed models have been proposed,[12,14–16] but these have typically focused on electronic applications and thus simplified the thermal considerations that are central to the present work.

The model is based on a modified potential field that allows for curvature:[13]

$$V(x)=-qF(L+R)\left[1-\frac{R}{x+R}\right]-\frac{q^2}{4\pi\varepsilon_0}\frac{K-1}{K+1}\frac{R}{(2R+x)2x}, \tag{3}$$

where q is the magnitude of electron charge, F is the applied field, L is the separation distance between electrodes, R is the characteristic radius of the emitter, ε_0 is permittivity of vacuum, K is the dielectric constant of the emitter, and x is the distance from the emitter. The total emission current, I, takes the form

$$I=qA\int_{-W_a}^{\infty}D(W)N(W)dW, \tag{4}$$

where $-W_a$ represents the bottom of the conduction band of the emitter. W is the x component of electron energy (i.e., in the dominant direction of emission), $N(W)dW$ is the electron supply function, and $D(W)$ is the quantum tunneling transmission coefficient. In the present work, the transmission coefficient is calculated using the Wentzel–Kramers–Brillouin (WKB) approximation

$$D(W)=\exp\left\{-\int_{x_1}^{x_2}\sqrt{\frac{8m}{\hbar^2}|V(x)-W|}dx\right\}, \tag{5}$$

where $V(x)$ is the energy profile of Eq. (3), x_1 and x_2 are the zeros of $W-V(x)$, and m is the electron mass. We recognize the limitation of the WKB approach to account properly for transmission at high fields and temperatures due to its approximate expansion about the chemical potential. However, its ability to capture trends and provide reasonable quantitative estimates of thermodynamic effects in a straightforward manner is the primary motivation for its use in the present work. The effect of small-scale features on emission current is included through the energy profile $V(x)$ in the transmission coefficient of Eq. (5). The supply function $N(W)$ can be formulated analytically[12] and is a function of emitter temperature and work function

$$N(W)=\frac{4\pi mkT}{h^3}\ln\left[1+\exp\left(\frac{\zeta-W}{kT}\right)\right]. \tag{6}$$

The integral current equation of Eq. (4), while lacking the convenience of an analytic form [such as the FN model of Eq. (1)], retains the full temperature dependence of field emission.

Consequently, the integral form is more physically accurate than the basic FN approach. In the present work, the integral was evaluated numerically to a convergence of less than 0.1%.

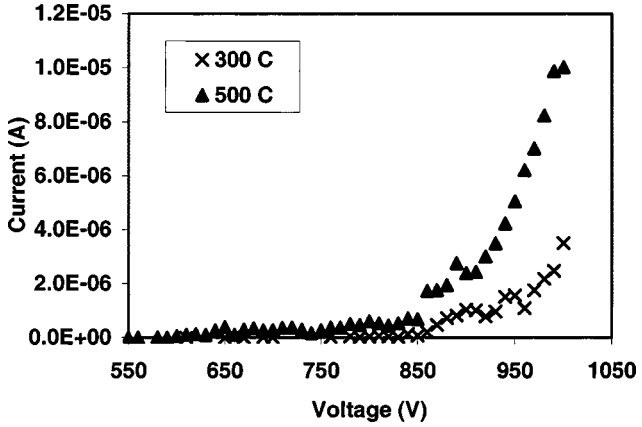

FIG. 1. $I-V$ behavior of n-type diamond cathode for temperatures $T=300$ and 500 °C.

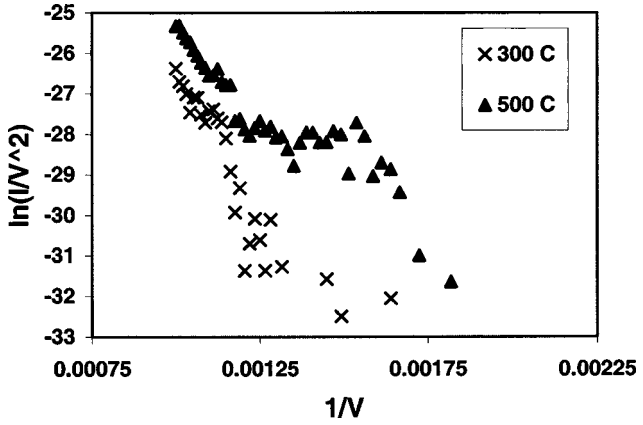

FIG. 2. FN plot of emission from an N-doped diamond cathode at $T=300$ and 500 °C.

III. PARAMETER ESTIMATION

Inverse techniques (and parameter extraction) can loosely be described as approaches for solving ill-posed problems.[17] The present problem can be described as ill-posed because experimental data inherently contain measurement errors. Therefore, the estimates will also contain errors. However, the error in the estimates can be characterized through the use of confidence intervals.[18] We note that field-emission experimental data are particularly noisy, and therefore, the use of the statistical estimation techniques is particularly appropriate. Parameter estimation techniques are related to curve fits (and actually reduce to curve fits for polynomial models), but can incorporate any forward model and measurement errors.

If the solution to a theoretical model [e.g., Eqs. (1) or (4)] is expressed as a function of the unknown parameter vector, which contains β, ϕ, and A for the FN model, and R, ϕ, and A for the alternate model, then the estimates can be found from a simple minimization problem. The objective, S, is given in terms of the experimental data, $\mathbf{Y}$, and the model solution, $\boldsymbol{\eta}(\boldsymbol{\gamma})$:

$$S=[\mathbf{Y}-\boldsymbol{\eta}(\boldsymbol{\gamma})]^T\boldsymbol{\Phi}^{-1}[\mathbf{Y}-\boldsymbol{\eta}(\boldsymbol{\gamma})], \tag{7}$$

where Φ is the covariance matrix of measurement errors. For simplicity, the covariance matrix is given as a square matrix with relative measurement errors for each measurement along the diagonal. If the error is constant, the matrix can be defined as the product of variance and the identity matrix. In this special case, measurement errors can be eliminated from the formulation because they do not affect the value of the estimates.

TABLE I. Total emission current and turn-on voltage data for the N-doped diamond cathode.

Temperature (°C)	Turn-on voltage (V)	Current at 950 V (A)
300	900	1.5×10^{-6}
500	860	5.1×10^{-6}

To determine the parameter vector $\boldsymbol{\gamma}$, the derivative of the objective function S with respect to the parameters vector is set to zero. In order to find this minimizer, the sensitivity of the model, $\boldsymbol{\eta}(\boldsymbol{\gamma})$, with respect to its argument $\boldsymbol{\gamma}$ must be calculated. The sensitivity matrix represents how the model changes with respect to the parameters, and is central to determining the parameter extraction process

$$\mathbf{X}=\frac{\partial\boldsymbol{\eta}(\boldsymbol{\gamma})}{\partial\boldsymbol{\gamma}}\approx\frac{\boldsymbol{\eta}(\boldsymbol{\gamma}+\boldsymbol{\delta\gamma})-\boldsymbol{\eta}(\boldsymbol{\gamma})}{\boldsymbol{\delta\gamma}}. \tag{8}$$

This matrix can be determined analytically in some rare instances; normally, it must be determined numerically. For example, the FN model of Eq. (1) has analytic derivatives in $\boldsymbol{\gamma}$. However, the derivatives of the alternate model of Eq. (4) are determined numerically by perturbing a single parameter $\boldsymbol{\delta\gamma}$, and using a finite difference approach.

Because the model will in general be nonlinear, we use a Taylor series expansion, neglecting higher-order terms to obtain an expression for the parameter vector correction:

$$\tilde{\boldsymbol{\gamma}}_{i+1}=\tilde{\boldsymbol{\gamma}}_i+\boldsymbol{\Delta\gamma},\quad \boldsymbol{\Delta\gamma}=\frac{\mathbf{X}^T\boldsymbol{\Phi}^{-1}[\mathbf{Y}-\boldsymbol{\eta}(\boldsymbol{\gamma})]}{\mathbf{X}^T\boldsymbol{\Phi}^{-1}\mathbf{X}}, \tag{9}$$

where the tilde represents the fact that the parameter vector is an estimate, and the subscript is an iteration index. The iteration process is continued until the objective defined by Eq. (7) is of the order of the variance of the noise in the measurements. If the number of measurements is greater than the number of parameters to be estimated, the data will not be matched exactly and we cannot expect to obtain an estimate that gives an objective less than the measurement noise. Also, because the objective is formulated as a least-squares minimization, we can be confident that a global minimum (excluding local noise minima) was found.

IV. EXPERIMENTAL SETUP

For this experiment, polycrystalline diamond samples were fabricated by plasma-enhanced chemical-vapor deposition on 2 in. silicon wafers.[19] The Si wafers were roughened with a diamond grit slurry to enhance the nucleation and growth of the diamond films. The samples were grown in

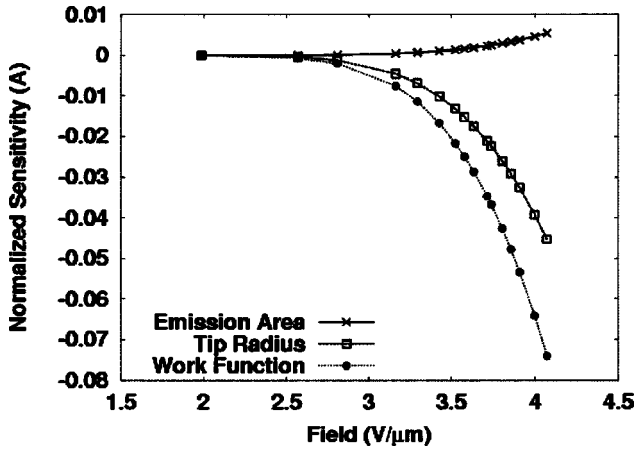

FIG. 3. Sensitivity coefficients as functions of applied field for the alternate model.

hydrogen plasma, with nitrogen gas added as a dopant source, to a thickness of 1.5 μm. To help activate the dopants in the diamond samples, rapid thermal annealing was utilized at 1000 °C. After the annealing process, the resistivity of the cathode was measured to be $\sim 1\ \mathrm{M}\Omega$ cm.

Field-emission properties were tested using a conventional diode method in a chamber evacuated to 10^{-7} Torr. A gold-coated copper sphere served as the anode, whose position was controlled by a micromanipulator. Molybdenum plates were used to provide the electrical contacts to the cathode and anode utilizing a 3000 W power supply (Sorensen DHP3U). An Agilent 34401A multimeter was used to record the emission current data through an IEEE-488 interface. The same sample was tested up to 1000 V at temperatures ranging from 300 °C to 500 °C. At each voltage increment, ten current measurements were taken to ensure consistency and repeatability. The average and standard deviation of the duplicate measurements also provide a statistical quantification of the measurement error due to noise.

A graphite heater block with two embedded resistive heaters served as the heat source to control the cathode temperature. Graphite was chosen due to its smaller coefficient of thermal expansion than the ceramic resistive heaters. Thus, good thermal contact was established between the graphite and the resistive heaters at elevated temperatures. To isolate the heater block electrically, an insulating sheet of aluminum nitride was used due to its high thermal conductivity. A tantalum heat shield was placed around the heater block to prevent radiative heat loss. Type K thermocouples were used for all temperature measurements.

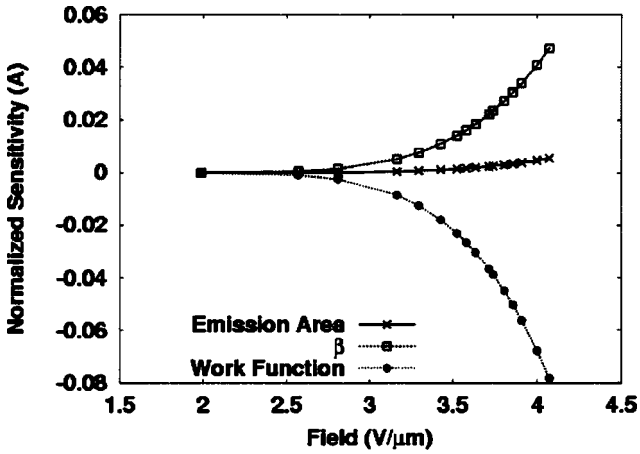

FIG. 4. Sensitivity coefficients as functions of applied field for the FN model.

V. RESULTS AND DISCUSSION

In Fig. 1, $I-V$ characteristics are shown for the N-doped CVD diamond sample on a Si substrate at high temperatures. Note that no emission was observed at room temperature. The data clearly indicate a strong dependence of field emission on temperature. The total emission current recorded at 950 V and the turn-on voltage at each temperature are shown in Table I. Higher total currents are observed with increasing temperature. The turn-on voltage was defined as the voltage required to reach 1 μA from the diamond sample. A significant reduction in the turn-on voltage is shown with increasing temperature. A FN plot for the emission data from the N-doped cathode is shown in Fig. 2. The characteristic linear trend with a negative slope indicates conformity to the FN relation [see Eq. (1)].

The results in Figs. 1 and 2 indicate a moderate temperature dependence, which can be explained by the increased carriers in the conduction band of the emitter. We postulate that the emission mechanism is similar to that proposed by Geis *et al.*[20] and others[21,22] and proceeds through three steps: (i) tunneling from the substrate to the diamond film, (ii) electron transport through the diamond bulk, and (iii) tunneling from the diamond surface to the vacuum. As temperature increases, the population of higher-energy electron grows, and more carriers can tunnel into the conduction band of the emitter. Neither the foregoing FN theory nor the alternate model is capable of simulating this complex emission process precisely. However, the estimated parameters, such as work function ϕ, field enhancement factor β, or characteristic radius R, provide some insight and correlation with the physical mechanism.

The linear dependence of the sensitivity coefficients indicates whether parameters are correlated. High correlation (or confounding) means that the parameters cannot be estimated independently. It has already been suggested that the parameters are highly correlated for the FN model because the formulation can be cast into an expression for a line. This form [Eq. (2)] contains, at most, two independent param-

TABLE II. Estimates of parameters from the alternate model with 95% confidence intervals.

Parameter	300 °C	500 °C
Emission area (μm^2)	$8.52e-6 \pm 1.59e-6$	$4.76e-4 \pm 1.20e-4$
Emission site radius (μm)	$9.30e-1 \pm 1.30e-1$	$5.23e-1 \pm 0.909e-1$
Work function (eV)	1.38 ± 0.121	2.26 ± 0.146

TABLE III. Estimates of parameters from the FN model.

Parameter	300 °C	500 °C
Emission area (μm^2)	$6.99e-6$	$9.00e-6$
Enhancement factor	32	41.3
Work function (eV)	1.14	1.27

eters. Figures 3 and 4 show the sensitivities of the current to the parameters to be extracted. A visual inspection suggests that all sensitivity coefficients exhibit possible linear dependent behavior. This feature can be verified further with the identifiability factor, which is found from the sensitivity matrix ($M=|X^TX|$). An identifiability of zero indicates perfect linear dependence. Therefore, any value greater than zero indicates a relative ability to extract unique parameters. Although the identifiability is arguably small in both cases ($M_{FN}=3.8e-27, M_{alt}=2.6e-19$), the alternate model clearly indicates an advantage over the FN model.

Because the three parameters of the FN formulation cannot be estimated simultaneously, we examine the alternate model first. This model is not strictly linear on a FN plot. Therefore, more than two parameters can be extracted simultaneously. Estimates of the parameters from the alternate model are given in Table II. For both temperatures, we expect the radius to be approximately the same since it is purely a geometric quantity. Although the estimates are slightly different, the difference is nearly within the measurement noise and the two are considered to be statistically similar. Despite the large confidence intervals on the area estimates, the difference here is significant. This difference is a function of the temperature of the device during emission. For elevated temperatures, the number of emission sites will increase. Because the emission area is related to the number of emission sites, the area should also increase. The estimates further indicate that the work function is a strong function of temperature. However, the estimates are comparable to the known work function of different forms of carbon.

The traditional FN approach for extracting parameters was also examined in an attempt to verify the estimates obtained from the alternate model. Even though we do not expect to be able to extract more than two parameters simultaneously, we can use the information obtained from the alternate model to guide the estimation of the FN parameters. The emission site radius and the enhancement factor are unique to the alternate model and the FN model, respectively. Therefore, these corresponding parameters cannot be compared directly. However, they are inversely proportional to each other; large field enhancement is a result of small emission site radius. The emission area and work function estimates are expected to be similar between the two models. Table III gives the estimates of the FN model. With the area fixed from the estimates of the previous analysis, the work function exhibits the same trend between temperatures. However, the values in each case are smaller than those estimated for the alternate model. The inverse relationship between the radius and enhancement factor was maintained.

VI. CONCLUSIONS

This work has presented experimental data for the field-emission characteristics of a N-doped CVD diamond cathode at elevated temperatures. The enhanced emission of thermally excited electrons allows field emission to be applied to power generation applications where high temperatures exist. An increase in the maximum current density and a decrease in the turn-on voltage were observed with increasing temperature.

Parameter estimation techniques, which provide a rigorous, statistical means of correlating experimental data with theoretical models, were applied to the problem of field emission and were shown to produce reliable results. From the alternate model, reasonable estimates for emission area, emission site radius, and work function were obtained simultaneously. The parameters extracted from the FN model verified trends found in estimates from the alternate model. All of the estimates indicate that the emission characteristics exhibit a strong dependence on temperature. Additional experiments should reduce the uncertainty in the parameter extraction process and improve the estimates.

Future work will concentrate on the temperature dependence of electron field emission for doped and undoped polycrystalline diamond structures. This work will provide insights into the high-temperature operation of a variety of field-emission devices. Also, a more comprehensive parameter estimation model will be developed to extract several physics-based parameters from experimental data.

ACKNOWLEDGMENTS

The authors gratefully acknowledge the support of the NSF CAREER Program (CTS-998361), NRO DII program (000-01-C-0230), and Vanderbilt University through its Discovery Grant program.

[1]T. S. Fisher and D. G. Walker, J. Heat Transfer **124**, 954 (2002).
[2]R. H. Fowler and L. W. Nordheim, Proc. R. Soc. London, Ser. A **119**, 173 (1928).
[3]C. A. Spindt, J. Appl. Phys. **39**, 3504 (1968).
[4]I. Brodie and P. R. Schwoebel, Proc. IEEE **82**, 1006 (1994).
[5]J. A. Nation, L. Schachter, F. M. Mako, L. K. Len, W. Peter, C.-M. Tang, and T. Srinivasan-Rao, Proc. IEEE **87**, 865 (1999).
[6]W. P. Kang, T. S. Fisher, and J. L. Davidson, New Diamond Frontier Carbon Technol. **11**, 129 (2001).
[7]J. Robertson, J. Vac. Sci. Technol. B **17**, 659 (1999).
[8]J. Ristein, F. Maier, M. Riedel, J. B. Cui, and L. Ley, Phys. Status Solidi A **181**, 65 (2000).
[9]L. Diederich, O. M. Keutel, P. Aebi, and L. Schlapbach, Surf. Sci. **418**, 219 (1998).
[10]P. K. Baumann and R. J. Nemanich, Surf. Sci. **409**, 320 (1998).
[11]J. B. Cui, M. Stammler, J. Ristein, and L. Ley, J. Appl. Phys. **88**, 3667 (2000).
[12]R. H. Good and E. W. Muller, *Field Emission, Handbuch der Physik* (German) (Springer, Berlin, 1956), Vol. 21, p. 176.
[13]T. S. Fisher, Appl. Phys. Lett. **79**, 3699 (2001).
[14]A. Modinos, *Field, Thermionic, and Secondary Electron Emission Spectroscopy* (Plenum, New York, 1984).
[15]K. L. Jensen and E. G. Zaidman, Appl. Phys. Lett. **63**, 702 (1993).
[16]K. L. Jensen, J. Vac. Sci. Technol. B **17**, 515 (1999).
[17]A. N. Tikhonov and V. Y. Arsenin, *Solutions of Ill-Posed Problems* (V. H. Winston and Sons, Washington, D.C., 1977).
[18]J. V. Beck and K. J. Arnold, *Parameter Estimation in Engineering and*

Science (Wiley, New York, 1977).
[19]A. Wisitora-at, W. P. Kang, J. L. Davidson, Y. Gurbuz, and K. V. Kerns, Diamond Relat. Mater. **8**, 1220 (1999).
[20]M. W. Geis, J. C. Twichell, and T. M. Lyszczarz, J. Vac. Sci. Technol. B **14**, 2060 (1996).
[21]J. Y. Shim, H. K. Baik, and K. M. Song, J. Appl. Phys. **87**, 7508 (2000).
[22]N. Koenigsfeld, B. Philosoph, and R. Kalish, Diamond Relat. Mater. **9**, 1218 (2000).